Catalytic Modification of Flammable Atmosphere in Aircraft Fuel Tanks

Thesis by

Inki Choi

In Partial Fulfillment of the Requirements

for the

Engineer's Degree

California Institute of Technology

Pasadena, California

2010

(Submitted June 7, 2010)

Acknowledgments

I would like to show my appreciation to my academic advisor Professor Joseph Shepherd. He advised me with his abundant experience and knowledge to overcome obstacles whenever I lost my way. His patience especially allowed me to learn lots of experimental knowledge and gave me a scientific attitude.

My thesis committee members, Professors Meiron and Blanquart gave me very instructive comments. Their comments were of great help for me to complete a more integrated thesis.

I am also thankful to my laboratory members. They kept helping me adapt myself to life at Caltech. I appreciate particularly Philipp Boettcher and Sally Bane who helped me in various ways to fulfill my goal with experimental experiences and techniques.

Finally, I really want to show my deepest thanks to my wife who assisted me sincerely throughout the years here at Caltech. She was strong and very supportive even though it was very difficult time for us to stay here.

Abstract

A facility for investigating catalytic combustion and measurement of fuel molecule concentration was built to examine catalyst candidates for inerting systems in aircraft. The facility consists of fuel and oxygen supplies, a catalytic-bed reactor, heating system, and laser-based diagnostics. Two supplementary systems consisting of a calibration test cell and a nitrogen-purged glove box were also constructed. The catalyst under investigation was platinum, and it was mixed with silica particles to increase the surface area available to react. The catalyst/silica mixture was placed in a narrow channel section of the reactor and supported from both sides by glass wool. The fuels investigated were n-octane and n-nonane because their vapor pressure is sufficiently high to create flammable gaseous mixtures with atmospheric air at room temperature. Calibration experiments were performed to determine the absorption cross-section of the two fuels as a function of temperature. The cross-section values were then used to determine the fuel concentration before the flow entered the reactor and after exposure to the heated catalyst. An initial set of experiments was performed with the catalytic-bed reactor at two temperatures, 255 and 500°C, to investigate pyrolysis and oxidation of the fuel. The presence of the catalyst increased the degree of pyrolysis and oxidation at both temperatures. The results show that catalytic modification of flammable atmospheres may yield a viable alternative for inerting aircraft fuel tanks. However, further tests are required to produce oxidation at sufficiently low temperature to comply with aircraft safety regulations.

Contents

List of Figures

List of Tables

Chapter 1

Introduction

1.1   Background

A major concern in aviation safety and aircraft design is the possibility of accidental ignition of flammable mixtures. This explosion risk can be mitigated by eliminating all sources of ignition, which may be practically impossible, or by ensuring that the mixture composition cannot be ignited by any source. The gas in the fuel tank ullage is one of the main concerns. For example, the National Transport Safety Board investigation pointed out that the explosion of the center wing fuel tank resulting from the ignition of the flammable atmosphere in the tank was the probable cause of the TWA Flight 800 accident in 1996 (NTSB, 2000). Currently, the installation of an inert atmosphere generation system on the fuel tank is required by the Federal Aviation Administration (FAA, 2008).

One inerting system currently in use is a hollow fiber membrane, which operates on the principle of selective permeability creating an output flow that is highly enriched with nitrogen (Air Weekly, 2010). The output stream is directed into the fuel tank, displacing the potentially flammable mixture in the fuel tank ullage and thereby lowering the oxygen concentration below the flammability limit. A single unit of the hollow fiber membrane system weighs approximately 400 lbs and requires either engine bleed air or a separate compressor for the high-pressure input into the bundle of membrane fibers (Air Weekly, 2010). The use of engine bleed air requires a heat exchanger and ductwork carrying air from the engine to the separation unit. These requirements stand in contrast to the goal in current aircraft design, which aims to reduce weight and complexity by eliminating heat exchangers and duct work by using electrical systems instead of bleed air. Hence, alternative methods for inerting fuel tanks are in development.

One such alternative is low-temperature catalytic oxidation, which converts the flammable fuel-air mixtures into inert products. The key idea is to use catalysts to initiate reactions between hydrocarbon and oxygen molecules producing carbon dioxide and water vapor, which are fed back into the fuel tank displacing the vapor in the ullage. In this manner, the overall composition in the fuel tank is moved outside the flammability region, which is a function of the relative proportions of

fuel, oxygen, and the inert gas such as nitrogen or carbon dioxide (Zabetakis, 1965). The range of flammable mixtures is in fact smaller when carbon dioxide is used as the diluent instead of nitrogen. The proposed catalytic reaction combines the effect of lowering the oxygen concentration with the flammability reducing effect of carbon dioxide over nitrogen.

A schematic diagram of a fuel tank with the catalytic reactor is shown in Figure 1.1a. The pressure in the fuel tank is equal to the ambient pressure outside the plane at all times. The proposed catalytic conversion system would be installed on the aircraft connected to the fuel tanks via supply and return lines, such that flammable gas is removed from the fuel tank ullage and replaced by the process products.

Figure 1.1b illustrates the process of initial inerting and composition changes for a typical flight on a standard flammability diagram (Zabetakis, 1965). Immediately after fueling the plane the composition may be flammable and the inerting system is turned on. The amount of diluent is increased by the catalytic conversion, which corresponds to changing the composition from the initial point to point A in Figure 1.1b. The concentration of fuel in the vapor is only a function of the temperature and overall pressure because the fuel consumed in the reaction is replenished from the liquid phase. During the climb to cruise altitude it is assumed that a homogeneous mixture of the gas in the ullage is vented so that the concentration of fuel is increased and diluent gas concentration is decreased, as shown by point B. At this point the gas should still be non-flammable in the fuel tank ullage. However, as the plane descends and pressure increases the mixture may return into the flammable region before which the catalytic modification system can be re-engaged and inert the fuel tank.
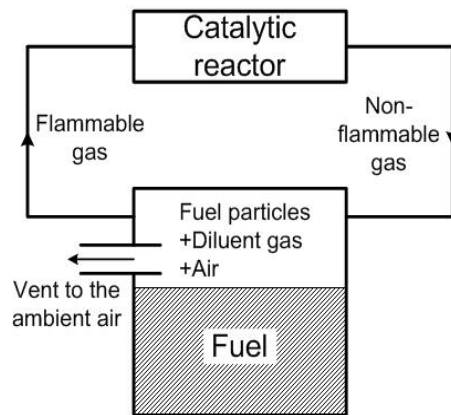
(a) Schematic diagram of the system with the fuel tank and the catalytic reactor
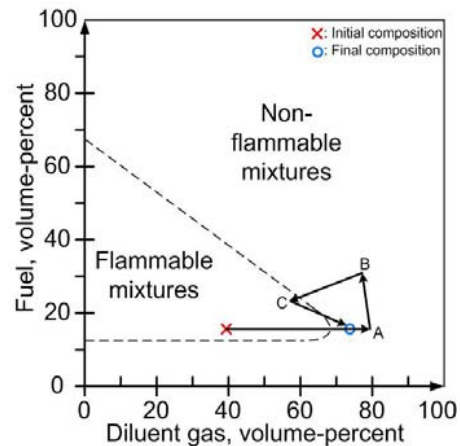
(b) Flammable region and the plan to treat the ullage gas in the tank

Figure 1.1: . Catalytic modification of flammable atmosphere in the aircraft fuel tank

Catalytic oxidation provides reaction pathways with lower energy barriers than conventional oxidation processes in flames. Thus, the temperature at which the oxidation takes place is significantly lower than flame temperatures, which is are typically on the order of 2000 °C (Heyes and Kolaczkowski, 1997). This technique is therefore potentially safer for use on aircraft in the fuel tank ullage or flammable leakage zones.

1.2   Objective

The main objective of this study is to develop an evaluation methodology and test metrics for screening catalysts that can be used for low temperature oxidation of jet fuel. The initial investigation was performed using a platinum catalyst in the laboratory using a bench-top experimental facility. The facility consists of precisely controlled fuel and oxygen supplies, a once-through catalytic bed reactor, a heated piping system, and laser-based diagnostics for measuring fuel concentration upstream and downstream of the reactor. Auxiliary systems include a calibration test cell and nitrogen-purged glove box for handling the catalyst.

Chapter 2

Theory

2.1 Catalytic Combustion

Catalytic combustion has been widely studied to understand the effect of the catalyst on the chemical pathways in the reactions. The catalyst promotes reaction pathways with lower energy barriers so that the fuel is burned at lower temperatures than in conventional combustion. Therefore, catalytic combustion is less hazardous because the system as a whole operates at significantly lower temperatures than in flames. Also, catalytic combustion can be achieved in fuel-oxidizer mixtures outside of the traditional flammability limits and can readily be studied in small-scale facilities (Heyes and Kolaczkowski, 1997).

The major products of catalytic combustion, referred to as total oxidation, are carbon dioxide and water vapor. Energy is released in the form of heat through the following overall reaction:

$$2C_xH_y + (2x + y/2)\,O_2 \rightarrow 2xCO_2 + yH_2O \tag{2.1}$$
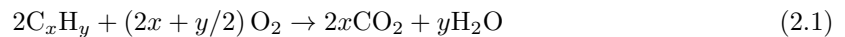
Due to the fact that the reactions occur at low temperatures, catalytic combustion produces less nitrogen oxides than traditional combustion (Heyes and Kolaczkowski, 1997). Therefore, catalytic combustion is a potential way to meet the increasingly strict emission regulations on industry and transportation. The performance of catalytic combustors depends on many parameters such as substrate structures, fuel-air ratio, catalytic material, and operating temperature.

Another reason that catalytic combustion is widely studied is that it provides a potential means of producing hydrogen for use as a fuel or in fuel cell systems. Hydrogen is produced through the partial oxidation reaction:

$$2C_xH_y + xO_2 \rightarrow 2xCO_2 + yH_2 \tag{2.2}$$

Fuel molecules can decompose through a process called pyrolysis, in which compounds undergo reactions without oxygen that only occur at high temperatures. The initial compound is transformed

into smaller molecules in these reactions (Moldoveanu, 1998). Pyrolytic reaction can be promoted by adding catalysts in what is called pyrolytic catalysis (Vasilieva et al., 1991).

Many previous studies on catalytic combustion have used methane as the fuel because methane has been widely used in transportation and power generation. Additional interest in catalytic combustion of methane has been prompted by its use in natural gas vehicles. Unburned methane in the exhaust gases poses an explosion hazard and may contribute to the greenhouse effect (Gelin and Primet, 2002).

2.2   Types of Catalysts

The noble metal catalysts, called the platinum group metals, have received attention for their high activity, excellent thermal stability, and lower tendency to react with support materials in comparison to base metals such as nickel (Ni), copper (Cu), cobalt (Co), manganese (Mn), and copper/chromium (Cu/Cr) (Gandhi et al., 2003). Noble metals outperform base metals in aspects of catalytic combustion such as intrinsic reactivity, durability, and poison resistance (Gandhi et al., 2003). In the platinum group metals, platinum (Pt), palladium (Pd), and rhodium (Rh) are preferred because ruthenium (Ru), iridium (Ir) and osmium (Os) all form volatile oxides which are impurities that have to be removed in a secondary process (Gandhi et al., 2003).

2.3   Ceramic Supporter

The enhancement of catalytic reaction by ceramic particles has been reported in previous studies [8, 9]. For methane combustion using Rh-based catalysts, the catalyst is most reactive when supported by aluminum oxide (Al_2O_3) and least reactive when supported by silicon dioxide (SiO_2), with titanium dioxide (TiO_2) being an intermediate ceramic. In addition to enhancing the reactivity, ceramics can also be used as a structural support. The ceramic provides a surface for spreading out the catalyst and thus increasing the surface area for reaction. Also, the ceramic particles can be mixed and packed together with smaller catalyst particles to allow more porosity for the fuel-air mixture to flow through.

2.4   Catalyst Geometry

There are geometric criteria that can be applied to a catalytic bed to increase its effectiveness. In this study, a once-through cylindrical catalytic bed is considered, where D_T is the cylinder diameter, L is the cylinder length, and D_P is the catalyst particle diameter. The first criterion that must be met is $D_T/D_P > 10$ to reduce the effect of channeling (Heyes and Kolaczkowski, 1997). Channeling

occurs when the majority of the flow travels through the single largest void in the packed catalyst bed. The second criterion is that D_T should be as small as possible to ensure uniform temperature while still maintaining an acceptable flow rate. As a compromise between the two criteria, the following geometry limitations are applied to the setup: $6 < D_T/D_P < 10$ and $50 < L/D_P < 100$ to reduce the effect of axial dispersion.

2.5 Laser Diagnostics

Laser diagnostics are often used in combustion research because they are non intrusive and provide fast response times to variations of species concentration. For example, laser absorption methods can be used to obtain the concentration of a hydrocarbon fuel. A helium-neon (He-Ne) laser omits light at a wavelength of 3.39 μm, which corresponds to the resonance wavelength of the C-H bond in a hydrocarbon molecule. Therefore, if the light from the He-Ne laser is passed through a gaseous medium containing hydrocarbon molecules, some fraction of the light will be absorbed by the C-H bonds and the intensity of the light will be reduced. The ratio of the observed light intensity, I, to the intensity without any fuel present, I_0, is related to the fuel concentration by Beer's law:

$$\frac{I}{I_0} = \exp\left(-\frac{\sigma_\nu P L}{\widetilde{R} T}\right) = \exp\left(-\frac{\sigma_\nu n L}{V}\right) \tag{2.3}$$

The symbols in Equation 2.3 are defined in Table 2.1. If the value of the absorption coefficient, σ_ν, is known, then the mole density of the fuel, n/V, can be determined from the intensity ratio. The absorption coefficient varies depending on the type of fuel, temperature, and pressure.

Table 2.1: Definitions and units of symbols in Equation 2.3

Parameter	Units	Description
I	AU	laser intensity
L	m	path length
n	mol	number of moles
P	atm	partial pressure
$\widetilde{R}$	atm m^3 mol^{-1} K^{-1}	universal gas constant
T	K	temperature
V	m^3	volume

Chapter 3

Experimental Setup

The experimental setup consists of 5 sub-systems and 2 auxiliary systems. Sub-systems include a piping system to deliver the gases, the pipe and flange heating systems, the gaseous fuel generating system, the catalyst-packed reactor inside a furnace, and the laser diagnostic system to measure fuel concentration upstream and downstream of the reactor. A calibration system and nitrogen-purged glove box were added as auxiliary systems. A schematic diagram of the setup is shown in Figure 3.1.
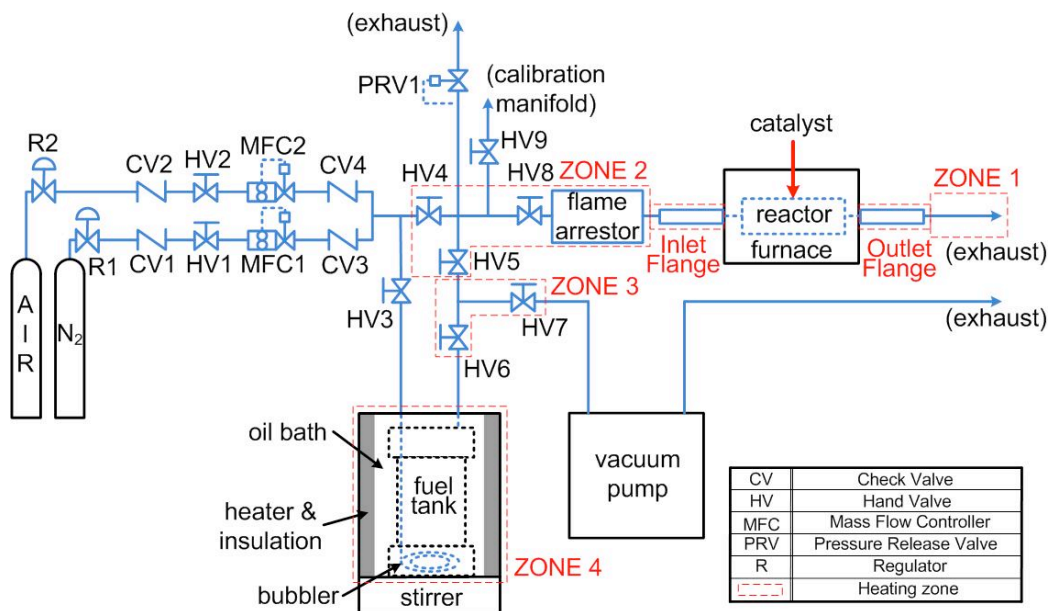
Figure 3.1: Schematic diagram of the experimental setup

3.1 Piping System

The piping system has two functions: supplying a gaseous fuel-air mixture to the reactor and venting the exhaust out from the setup. The amounts of nitrogen and air supplied to the reactor are controlled by two mass flow controllers (MFCs), which are operated remotely with a computer

using National Instruments LabVIEW software. The RS-232 DB-9 serial port on the computer is connected to an 8-pin mini-DIN connector on the mass flow controllers. Using the supply system, the air can be diluted with nitrogen to examine the effect of varying the oxygen concentration. The mass flow controllers and their connections to the piping system are shown in Figure 3.2.

Figure 3.2: The mass flow controllers connected to the piping system

Check valves were installed to prevent flow reversal, and a pressure relief valve prevents over-pressuring of the piping by venting the flow to the exhaust. A flame arrestor protects the fuel and air supplies from flashback. It is possible to change the route of the flow several ways using seven hand valves. For example, the flow can contain fuel molecules or only air through use of hand vales 3 and 5. After every test, the system is evacuated using a vacuum pump with hand valves 3, 4, and 6 closed and valves 5, 7, and 8 open to remove any remnant fuel.

The exhaust system is shown in Figure 3.3a. The mounted fan draws any gas leaking from the system through an exhaust hood mounted over the furnace to the exterior of the building. The exhaust gases from the vacuum pump and the experiment plumping are passively vented. The gas from the outlet of the reactor flows through the exhaust line and is vented out of the room. Any fuel vapor that has condensed will accumulate at the bottom of a tee built into the exhaust line. The fuel can then be drained from the tee after the experiment, as shown in Figures 3.3a and 3.3b.

3.2 Gaseous Fuel Generating System

The fuel vessel is shown in Figure 3.4c. A bubbler is made from quarter-inch tubing formed into a spiral with small holes approximately 1 mm diameter and is submersed in the fuel. Bubbling

(a) Exhaust line tee and funnel
(b) HDPE tube and bucket
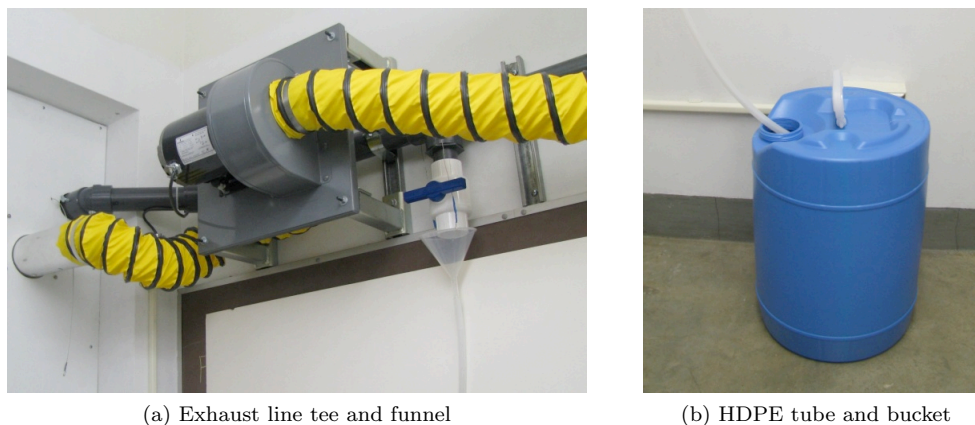
Figure 3.3: Gas exhaust fan and exhaust lines and condensed fuel removal system in the exhaust line

air through the fuel creates a fuel-air mixture supplied to the catalytic reactor. Flash point and vapor pressure measurements are used to characterize the fuel volatility (Reid et al., 1987, Kuchta, 1985). By controlling the fuel tank temperature, the vapor pressure can be varied to change the fuel concentration in the mixture. The vessel sits on a magnetic stirrer platform that agitates the liquid to prevent stratification of multi-component mixtures and to ensure temperature uniformity in the fuel. The stirring bar inside the vessel was manufactured with a ring to ensure stable rotation.

(a) Stirring bar with ring
(b) Bubbler
(c) Fuel vessel
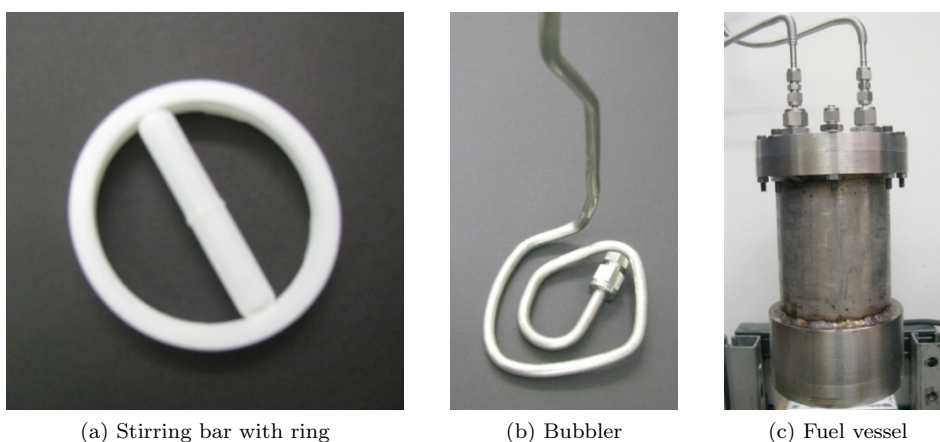
Figure 3.4: The fuel vessel, with stirring bar, and bubbler setup for creating fuel-air mixtures

The liquid fuel temperature is regulated by immersing the vessel in an ethylene glycol bath that is constantly circulated by a pump. The fuel heating system system is shown in Figure 3.5. Four tape heaters are attached to the outer wall of the bath using heat-conducting glue. The walls of the bath are covered with a glass-fiber insulating jacket. The bath is placed inside a structure with four support pillars to prevent the bath from tipping over.

(a) Thermal bath   (b) Fuel vessel in heating bath   (c) Circulation pump
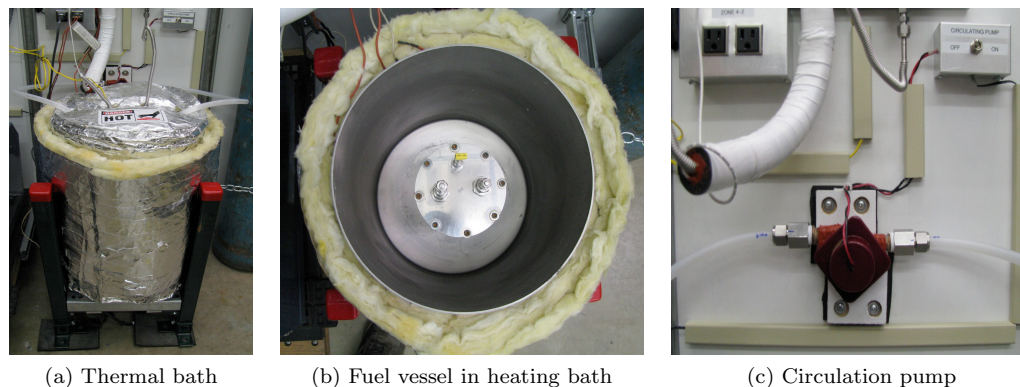
Figure 3.5: Gaseous fuel generation system

3.3 Heating System

3.3.1 Pipe Heating System

A heating system, required to keep heavy hydrocarbon fuels from condensing, is installed on the piping system. The heavier the hydrocarbon, the lower the vapor pressure at a specific temperature. Therefore, heavier hydrocarbons condense more easily than lighter hydrocarbons at the same temperature. Because condensation can change the concentration of fuel molecules in the flow going into the reactor, the fuel must remain completely gaseous. To ensure that the fuel is in the gas phase, the heating system is used to maintain the temperature of the piping system above the boiling point of the test fuel. The heating system consists of four zones controlled independently using the heater control panel shown in Figure 3.6. A circuit breaker box is located under the control box to cut off the power in case of emergency. This box also controls the power to the other facilities such as the furnace, the laser system, the stirrer, and the circulation pump.

(a) Pipe heating system control panel   (b) Control panel wiring
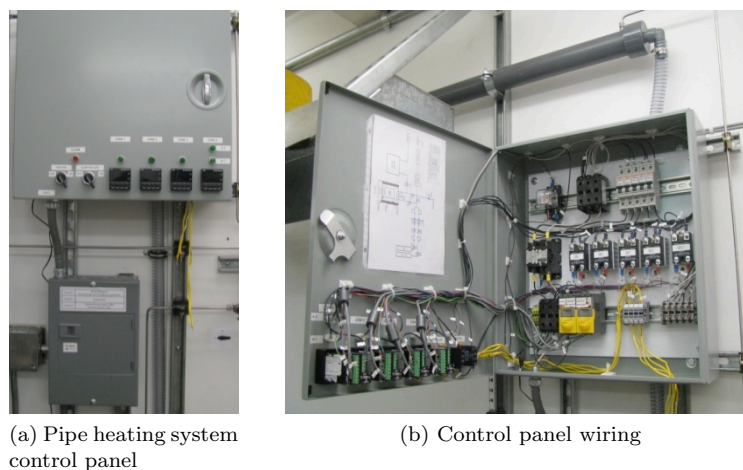
Figure 3.6: Control panel for the pipe heating system

The control system includes an alarm circuit that shuts down all heaters in the event that the temperature exceeds safe operating conditions. The control panel is comprised of the heater circuit and the alarm relay circuit, schematics of which are shown in Figure 3.7. To initiate operation, the controller switch is closed supplying 120 VAC power to the controllers. In normal operation the alarm contacts in the controllers are all closed so that closing the heater switch energizes the 9 VDC circuit to place the alarm relay in the "safe" condition. This action turns off the red alarm indicator light and activates the contactor that passes AC power to the heaters. Once the contactor is closed, the controllers supply the appropriate control signal to the solid state relays that switch the power to the heaters. The heaters are connected in series with circuit breakers. When power is supplied through the solid state relays to the heaters, a green indicator light is on. As long as the temperature remains within the acceptable rage, the alarm light remains off and power is supplied to the heaters. Manual toggling of the heater switch or tripping of any alarm in the controllers results in switching the alarm relay to the "alarm" condition. This opens the main contactor, removing power to the heaters while simultaneously illuminating the red alarm indicator light.

A serious problem had to be resolved to get this control system operational. The transients induced by switching of contactor had to be isolated from the power supplied to the controllers, since these transients caused the controllers to become unstable. This issue was overcome by introducing a diode across the alarm relay, running the alarm circuit with a separate 10 VDC power supply, and adding ferrite beads to the controller power supply lines and control signal wiring.

The piping system is divided into four heating zones to allow for maximum control of the temperature. Rope heaters are wrapped around the pipe, and heated to prevent gaseous fuel from condensing in the piping system. Silicon insulating jackets cover the pipe and heaters to minimize heat loss as shown in Figure 3.8. The gaps between the jackets are filled with silicon-based sealant, and white heat-resistant tape encapsulates the insulating jackets. Metal and Teflon-based hand valves are used with extension rods in the heating zones because plastic-based valves cannot endure temperatures over 150°C. Four thermocouples are taped to the surface of the pipe to measure the temperatures of the four heating zones. The thermocouples are positioned some distance away from the rope heaters so they do not become hotter faster than the piping. The temperatures from the thermocouples are read by the heater controllers, which switch solid state relays to power the heaters.

3.3.2 Flange Heating System

A second heating system is required for the flanges because gaseous fuel can condense at the flanges where the sapphire windows are exposed to the ambient air. Rope heaters wrapped around the inlet and outlet flanges are operated by a control panel that is also composed of an alarm relay circuit and heater circuit, as shown in Figures 3.9 and 3.10. The heater circuit is operated in the same

(a) Alarm circuit
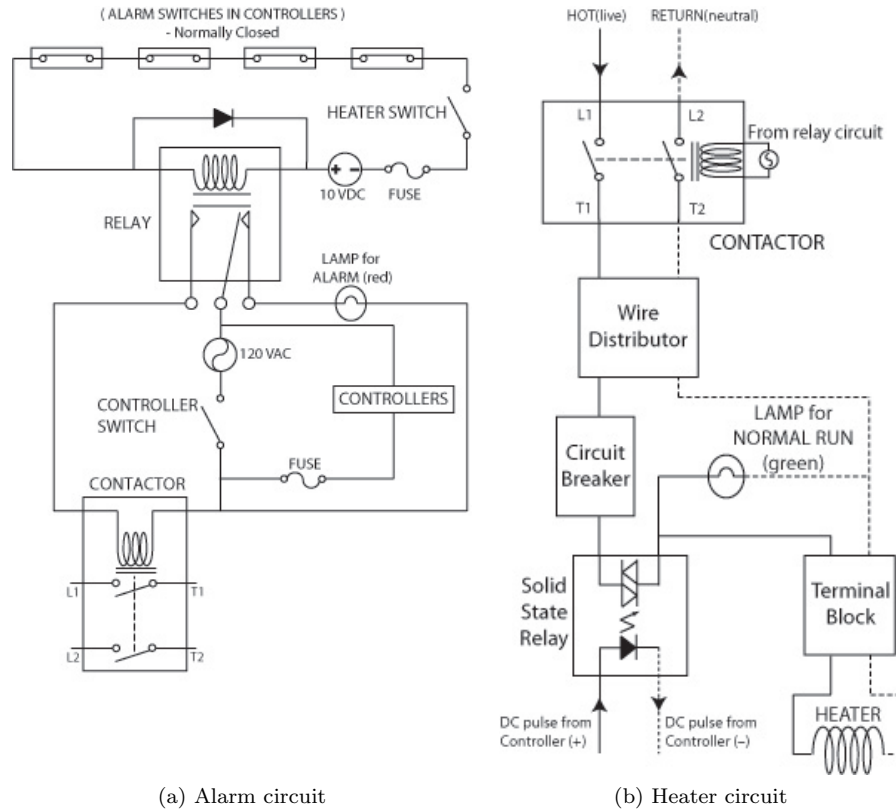
(b) Heater circuit

Figure 3.7: Circuit diagrams for the piping heating system

way as that of the piping heating system. However, the alarm relay circuit for the flange heaters is slightly different. The contacts in the controllers are normally open as long as the temperature stays within the safe range. Therefore, the alarm light will remain off and the heater circuit will be powered through the contactor. If the temperature exceeds the same limit as the pipe heating system, the contacts will be closed and the alarm light will be on, cutting off the power to contactor.

The quartz reactor tube is longer than the furnace, and so rope heaters are used to heat the exposed ends of the tube as shown in Figures 3.11a and 3.11b. Aluminum faced fiberglass insulation covers the flanges and two ends of the reactor. The sapphire windows are not covered because they are used as the pathway through the reactor for the HeNe laser beam. Two thermocouples are taped to the surfaces of the flanges to read the temperature as inputs to the heater controllers. Two additional thermocouples are inserted through the top of the flanges to measure the temperature of the gas just above the laser path. Figure 3.11c shows the enlarged sapphire window which is exposed to the ambient air. The head of the thermocouple can be seen through the window.

(a) Piping system gas inlet

(b) Piping system hand valves

(c) Piping system outlet
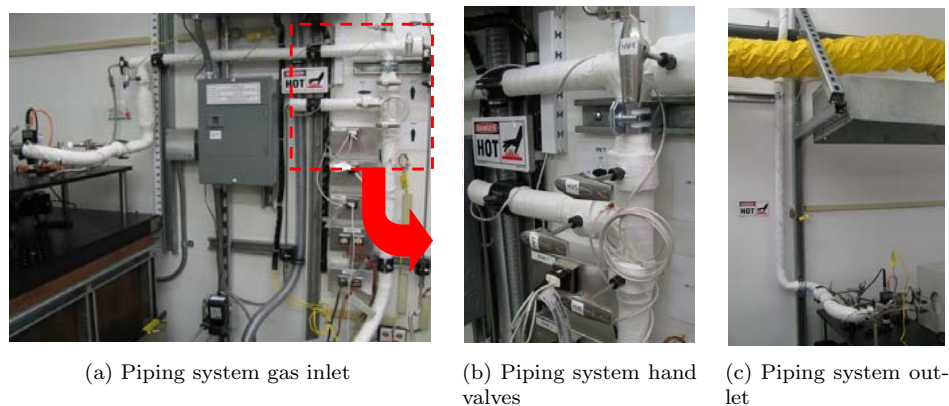
Figure 3.8: Heating and insulation system for the gas piping system

(a) Flange heating system control panel

(b) Control panel wiring
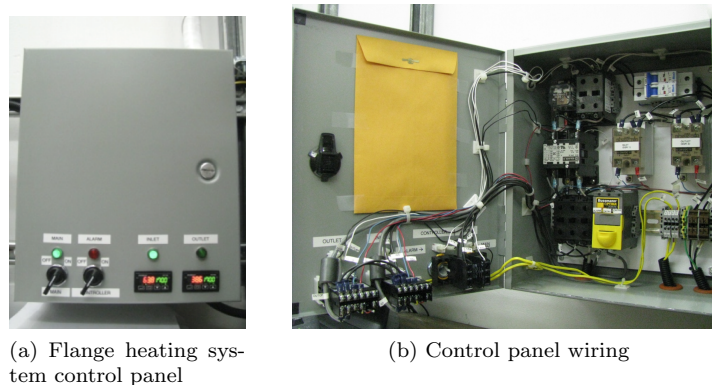
Figure 3.9: Control panel for the flange heating system

3.4   Catalyst-Packed Reactor

Figure 3.12 shows the details of the reactor and the inlet/outlet flanges. The catalytic materials are contained in a quartz tube which can be heated up to 1100°C in the furnace. Two flanges on the end of the reactor are connected to the piping system and ease the removal of the reactor when the catalytic material is changed. The flanges also hold the optical ports with the sapphire windows that provide the pathway through the reactor for the laser beam. The length of the pathways, i.e. the internal distance between the sapphire windows, are 43 mm and 41 mm for the inlet and outlet flanges, respectively. A length of approximately 1 ft in the middle of the reactor is heated by a furnace to temperatures sufficient to initiate catalytic reaction. The furnace is controlled by a built-in PID circuit with the input from a thermocouple located beside the narrow middle section of the reactor, as shown in Figure 3.12.

The sapphire windows are mounted on short lengths of tube made of Schott specialty glass. The tubes are connected to the reactor flanges using ball and socket joints to protect the glass from

(a) Alarm circuit (b) Heater circuit
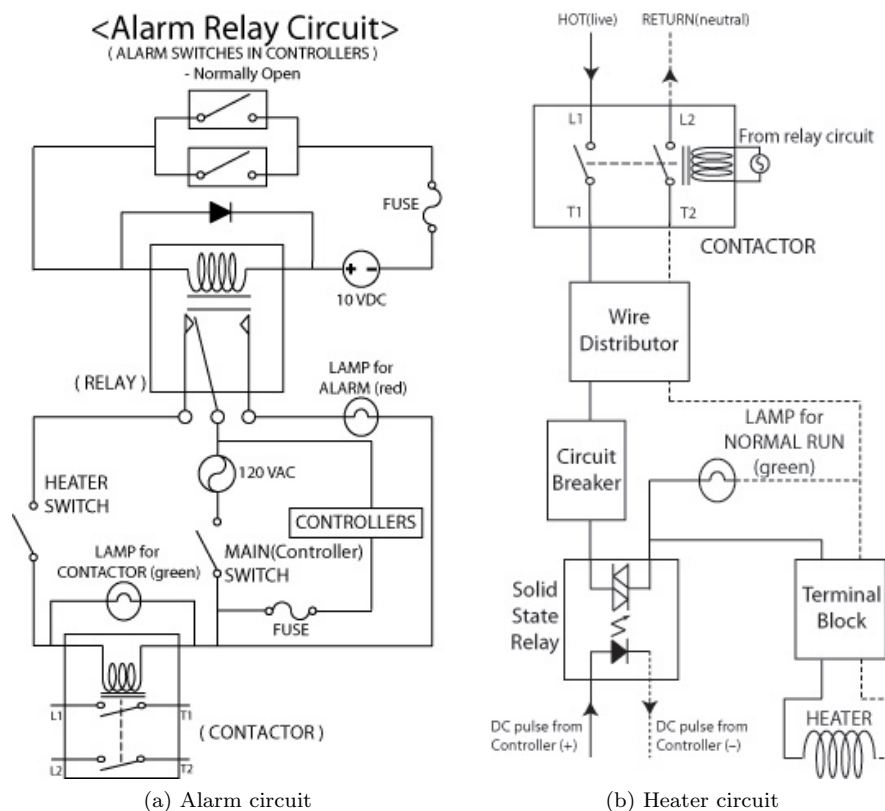
Figure 3.10: Circuit diagrams for the flange heating system

(a) Reactor tube inlet (b) Reactor tube outlet (c) Sapphire window
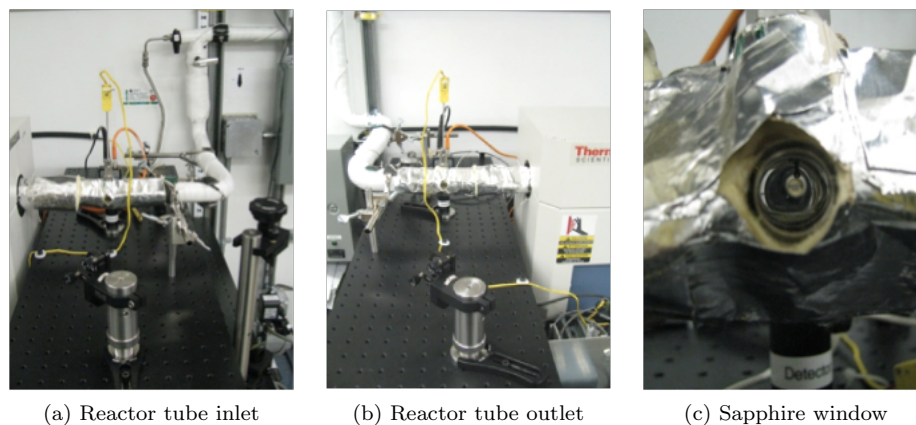
Figure 3.11: Heating and insulation system for the reactor flanges

breaking and for ease of replacement. Since the thermal conductivity of quartz is low, this method of construction is acceptable for the flanges because they are more than 2 inches away from the furnace. For heavy hydrocarbons such as n-octane and n-nonane, the absorption cross section was found to be dependent on temperature, but there is negligible dependence on pressure (Klingbeil et al., 2006). Therefore, only the gas temperature is needed at the inlet and outlet flanges. So
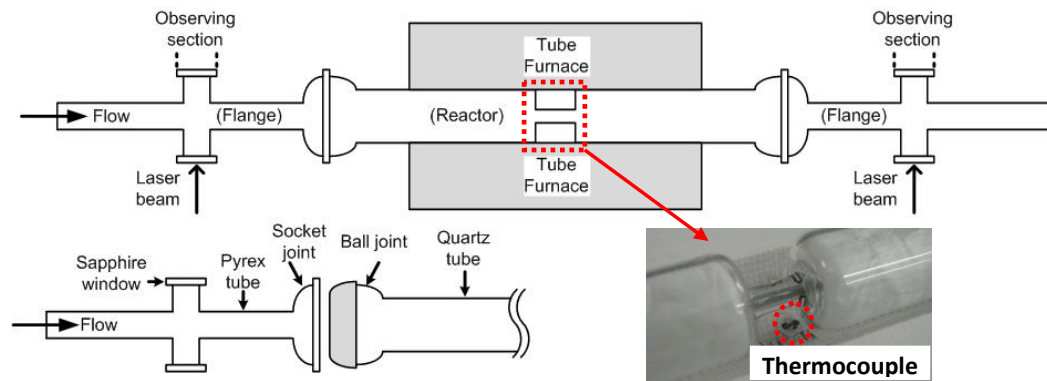
Figure 3.12: Reactor assembly

thermocouples are mounted in the flanges with the thermocouple junctions located just above the path of the laser beam. The flanges are connected to the gas supply and exhaust system using flexible tubes to protect the glassware from mechanical strain. The catalyst is placed in a narrow channel in the middle of the reactor, as shown in Figure 3.13. The catalytic material is packed in the channel and held in place by pushing glass wool into the reactor from both ends.
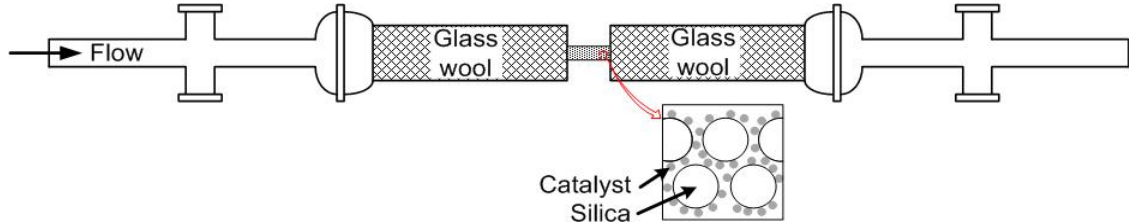
Figure 3.13: Catalytic bed

3.5   Laser Diagnostics

The optical system consists of a HeNe laser, a filter, a chopper, mirrors, a beam splitter, and detectors for measuring fuel concentration. The laser, chopper, and filter are mounted on a lower optical table, and mirrors are used to steer the laser beam up to a higher optical table at the same vertical height as the reactor. The beam is then split so that it goes through the optical ports both upstream and downstream of the furnace and finally reaches the detectors, as illustrated in Figures 3.14 and 3.15. The other experimental facilities, such as the piping system and heater control panel, are shielded from the experiment by movable aluminum plates.

The laser beam intersects the sapphire windows at a slight angle to avoid interference effects.
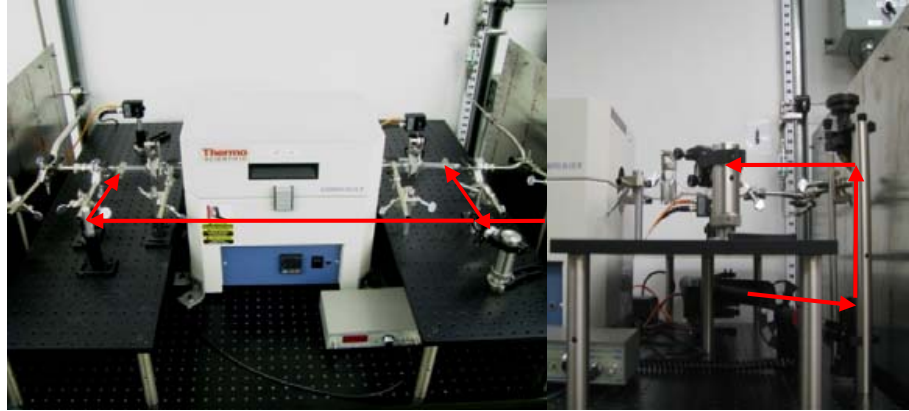
Figure 3.14: Optical system for laser-based fuel sensing
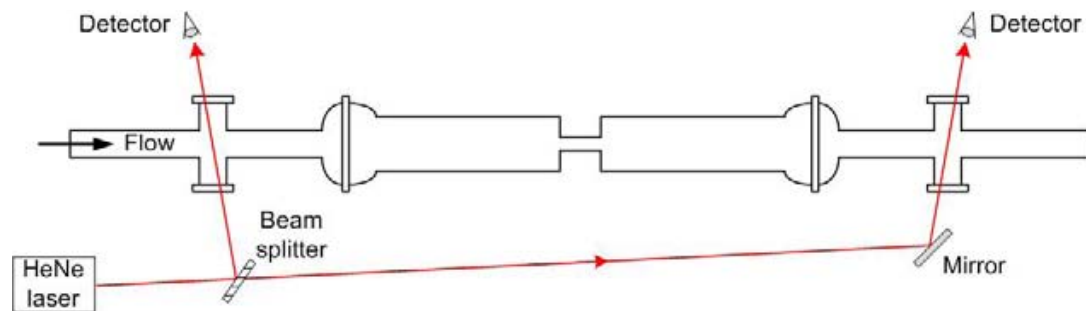
Figure 3.15: Schematic view of the optical setup

When the flange temperature is increased, the thermal expansion of the sapphire windows and flanges result in a change in the thickness of each window and the path length between the windows. The changes in the path length due to thermal expansion are of negligible magnitude, and are therefore neglected in this investigation. The changes in thickness of the windows cause a change in the interference patterns internal to the window, but this effect is accounted for by taking reference measurements at each temperature.

The alignment of the laser is done by following the faint plasma glow and observing the detector signals in LabVIEW. The room windows are covered with black panels to reduce the ambient light level in the room during alignment of the optics. The output from the two detectors and the reference laser signal from the chopper are digitized and then analyzed using LabVIEW software. A screen shot of the LabVIEW virtual instrument is shown in Figure 3.16.

A narrow band-pass filter (68 nm FWHM) is introduced to improve the quality of the laser source. The filter is placed between the chopper and the mirror as shown in Figure 3.17a. The filter is necessary because the HeNe laser source also emits a diffuse glow and light at wavelengths other than 3392 nm, which could alter the reading of the detectors. The filter removes wavelengths that are not within a certain tolerance of 3392 nm, as shown in the transmittance plot in Figure 3.17b.
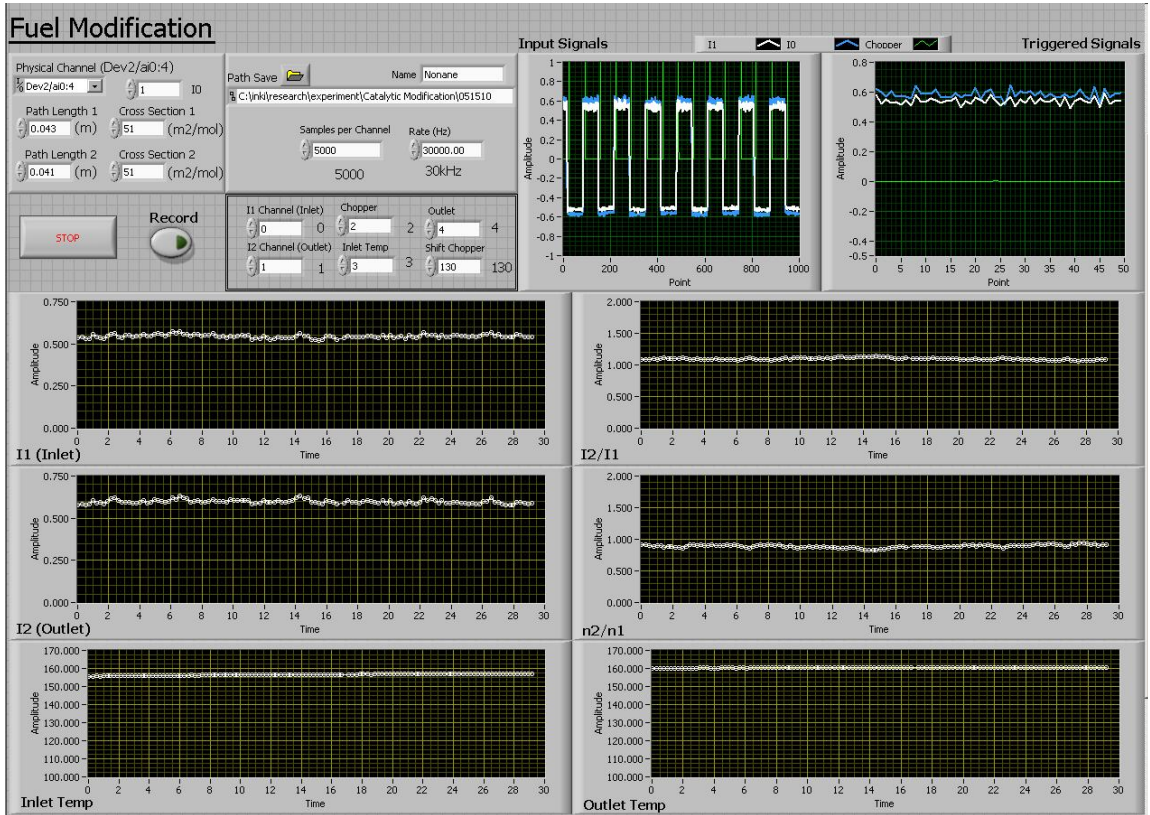
Figure 3.16: Screen shot of the LabVIEW virtual instrument used for fuel concentration measurements
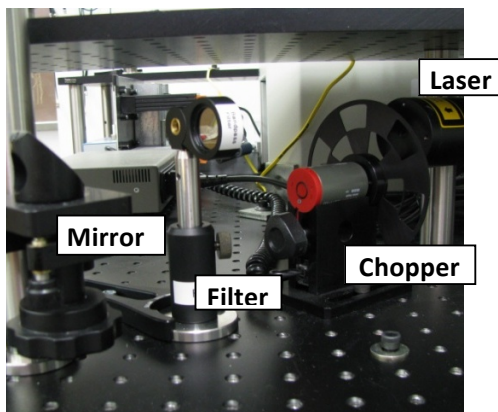
(a) Filter between the chopper and the mirror
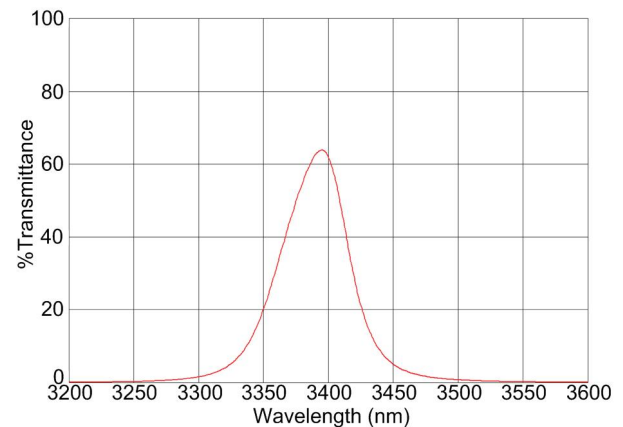
(b) Transmitting characteristic of the filter (reproduced from Infrared Optical Products, Inc. documentation)

Figure 3.17: Infrared filter

3.6   Auxiliary Systems

3.6.1   Calibration System

To determine the absorption cross-section values accurately over a range of temperatures, a calibration system was added to the original piping system. The system consists of a test cell with two sapphire windows, a pressure gauge, septum, and hand valves as shown in Figure 3.18. The leak rate of the calibration system was determined to be only 650 μTorr/min. The calibration system is connected to hand valve number 9 of the piping system using a flexible tube, allowing for the cell and tubing to be evacuated by the vacuum pump before each test. A rope heater is wrapped around the cell as well as the pressure gauge and septum. An aluminum-faced fiberglass insulation jacket and silicon insulation with heat-resistant tape is used to cover the system. There are two thermocouples in the test cell. One thermocouple is on the surface of the cell to read the cell temperature as an input to the controller, and the other thermocouple is mounted inside the cell just above the path of the laser beam to measure the gas temperature. The laser beam is split, with one beam passing through the cell and the other passing outside the cell. Two detectors measure the reference laser intensity and the variation of the beam after it passed through the test cell.
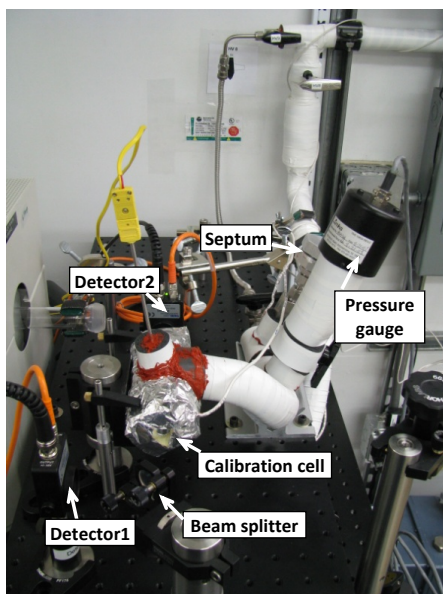
Figure 3.18: Calibration system

3.6.2   Glove Box

Another safety feature that was added to the facility is a glove box to use when handling the catalysts, shown in Figure 3.19. By using the glove box, catalysts are isolated from any sources of ignition and any flammable atmosphere since the glove box is purged with nitrogen. Dust from a

catalyst such as platinum sufficient concentrations can form explosive mixtures with air if there is a sufficient concentration. Additionally, using the glove box prevents the operator from being exposed to catalyst dust during packing. Neoprene gloves are used that are compatible with the candidate catalysts. A digital balance with a 0.001 g resolution is used to measure the mass of the catalyst and is operated inside the glove box. Before every operation, the glove box is purged with N_2 gas from the inlet in the left side of the box, forcing the air out of the gray pipe in the right corner of the box. The glove box is fixed on the table using wooden frames at the base.

A glass funnel and wooden support frame were constructed to aid in packing the catalyst into the reactor. The funnel has a sharp end tip with a 1 mm inner diameter so that it can be placed precisely between the narrow section and the end of the reactor while packing the catalyst. The support frame holds the reactor in place while packing.
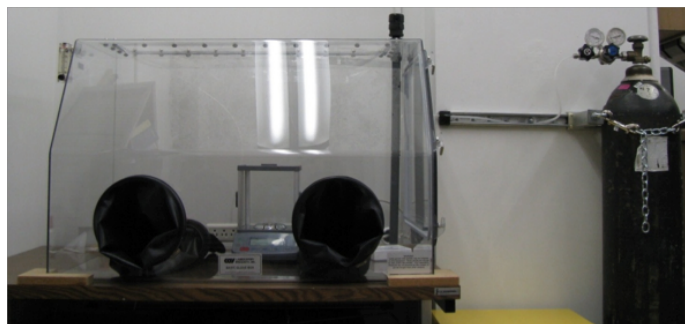
Figure 3.19: Glove box used when handling the catalyst

(a) Support frame

(b) Glass funnel

Figure 3.20: Catalyst packing system

Chapter 4

Experimental Procedures

4.1 Catalyst Preparation

The catalyst was prepared by mixing the platinum particles with the supporting silica in a ball mill with zirconia spheres. The platinum powder has a purity of 99.9% and 0.15-0.45 μm particle size. Silica particles, which are 99.8% pure and have a particle size of 0.1-0.5 mm, were washed and calcined by the manufacturer. All materials were procured from Sigma-Aldrich.

The catalyst particles, silica particles, and zirconia spheres were all placed in a vial and distilled water was added. The mixture of silica and platinum (1% platinum by weight) was mixed on a ball mill for 24 hours to create a homogeneous mixture. The zirconia spheres served to break up larger lumps of particles. The initial catalyst mixture preparations are illustrated in Figure 4.1.

The mixture was then dried in the N_2-filled glove box. In order to separate the catalyst, a mortar was covered with plastic wrap that was punctured with a series of holes that were smaller than the zirconia spheres (see Figure 4.2). The final catalyst mixture in the mortar was ground by a pestle to ensure that the catalyst mixture was fully homogeneous. The final preparation steps for the catalyst mixture are illustrated in Figure 4.2.

4.2 Catalyst Packing

The catalyst was packed into the reactor inside the N_2-filled glove box. First, one side of the reactor was filled with Pyrex glass wool procured from Corning. Then, the reactor was placed on a supporting frame with the glass funnel inserted in the empty end as shown in Figure 4.3. The catalyst material was poured into the funnel until the narrow middle section of the reactor was filled. The mass of the catalyst material used was carefully measured using the balance during the filling process. Finally, the second end of the reactor was packed with glass wool.

(Pt catalyst: 0.10~0.45μm) (Silica: 100~500 μm) (Zirconia balls, O.D: 1/8 in)
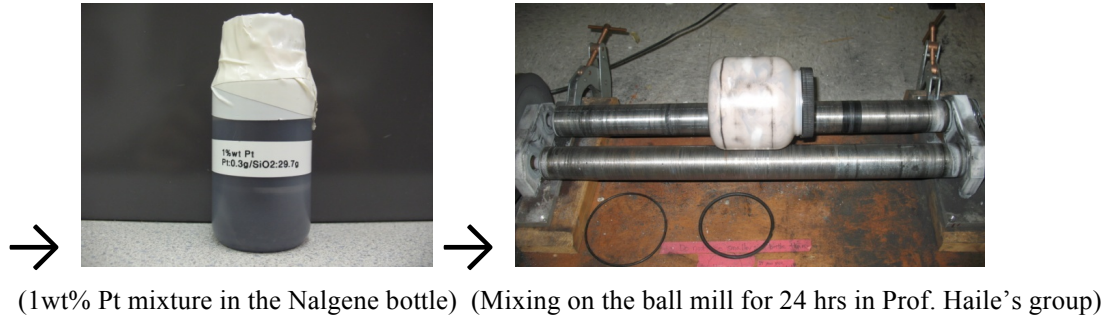
(1wt% Pt mixture in the Nalgene bottle) (Mixing on the ball mill for 24 hrs in Prof. Haile's group)

Figure 4.1: Initial catalyst mixture preparation

4.3 Calibration

For heavy hydrocarbons such as n-octane and n-nonane, the absorption cross-section was found to be dependent on temperature but there is negligible dependence on pressure [10]. Therefore, calibration of the absorption cross section as a function of temperature was necessary.

The calibration experiment proceeded as follows. First, the manifold was heated up to a pre-selected temperature where the cross-section value was to be determined. Then, the test cell was evacuated and the hand valve was closed to quarantine the cell from the vacuum manifold. Next, a small amount of fuel is injected into the test cell using a micro-liter syringe. The molar density of the fuel in the cell was calculated from the pressure and the temperature. After determining the molar density, the laser intensity was recorded. The intensity of the beam through the cell was measured while fluctuations of the laser baseline intensity were accounted for by the use of a reference detector via a beam splitter. From the ratio of these two laser light intensities the cross-section value at a given temperature could be calculated using Beer's law:

$$-\frac{1}{L}\left(\log\frac{I}{I_0}\right) = \frac{P}{\widetilde{R}T}\sigma_\nu = \frac{n}{V}\sigma_\nu \ . \tag{4.1}$$

Tests were performed at 23, 125, 150, 175, and 200°C, and at each temperature, measurements were taken with 5 or 6 different concentrations of the fuel. The fuel concentration, n/V, was known

from the fuel partial pressure and the temperature,

$$\frac{n}{V} = \frac{P_{fuel}}{\widetilde{R}T} \ .$$
(4.2)

Following Equation 4.1, the calculated values of the quantity $-1/L \left(\log \left(I/I_0 \right) \right)$ were plotted versus the fuel concentration. An example of such a plot for octane at $200°C$ is given in Figure 4.4. A linear fit was performed on the data, and the slope of the trend line was taken to be the absorption cross-section, σ_ν. The absorption cross-section could be calculated from a single fuel concentration measurement. However, calculating the cross-section using the method described here provides a greater degree of confidence in the results.

4.4 Catalytic Modification

With the knowledge of the fuel's absorption cross-section as a function of temperature from the calibration experiments, the fuel concentration could be calculated from the ratio of observed laser intensities:

$$\frac{n}{V} = -\frac{\log \frac{I}{I_0}}{\sigma_\nu L}$$
(4.3)

Finally, the variation of fuel concentrations between locations upstream and downstream of the catalyst could then be estimated:

$$\frac{\Delta n}{V} = \frac{n_1 - n_2}{V} = -\frac{1}{\sigma_\nu L} \left(\left(\log \frac{I_1}{I_0} \right) - \left(\log \frac{I_2}{I_0} \right) \right) = \frac{\log \frac{I_2}{I_1}}{\sigma_\nu L}$$
(4.4)

4.5 Test Procedure

Before the test, the boiling temperature of the fuel was identified as this is the minimum temperature for the system during operation to ensure that the fuel remains gaseous. While the piping system and reactor flanges were heating up to the boiling temperature, nitrogen gas was flowing through the reactor. During this time, the furnace was also heated to $255°C$. After heating, the gas flow was switched from nitrogen to air, and baseline laser measurements were taken. Then the gas flow was changed again to fuel and air to check for any low-temperature reaction. The furnace temperature was then increased to $500°$, and during the heating time the flow was switched to fuel and nitrogen. Using nitrogen instead of air prevents oxidation during the heating process, however, fuel pyrolysis may still take place. Once the temperature reached equilibrium, the nitrogen was replaced with air to test oxidation of the fuel. Then the flow switches back to fuel and nitrogen to check for pyrolysis at the high test temperature. Finally, the flow was changed to pure nitrogen to ensure that the laser measurements return to their baseline values.

(Drying in N$_2$-filled glove box)

(Removing zirconia balls using plastic wrap)

(Zirconia balls left on the wrap) (Grinding Pt mixture using a mortar and a pestle)

(Final state of Pt-silica mixture)

Silica → Pt ←

100 µm
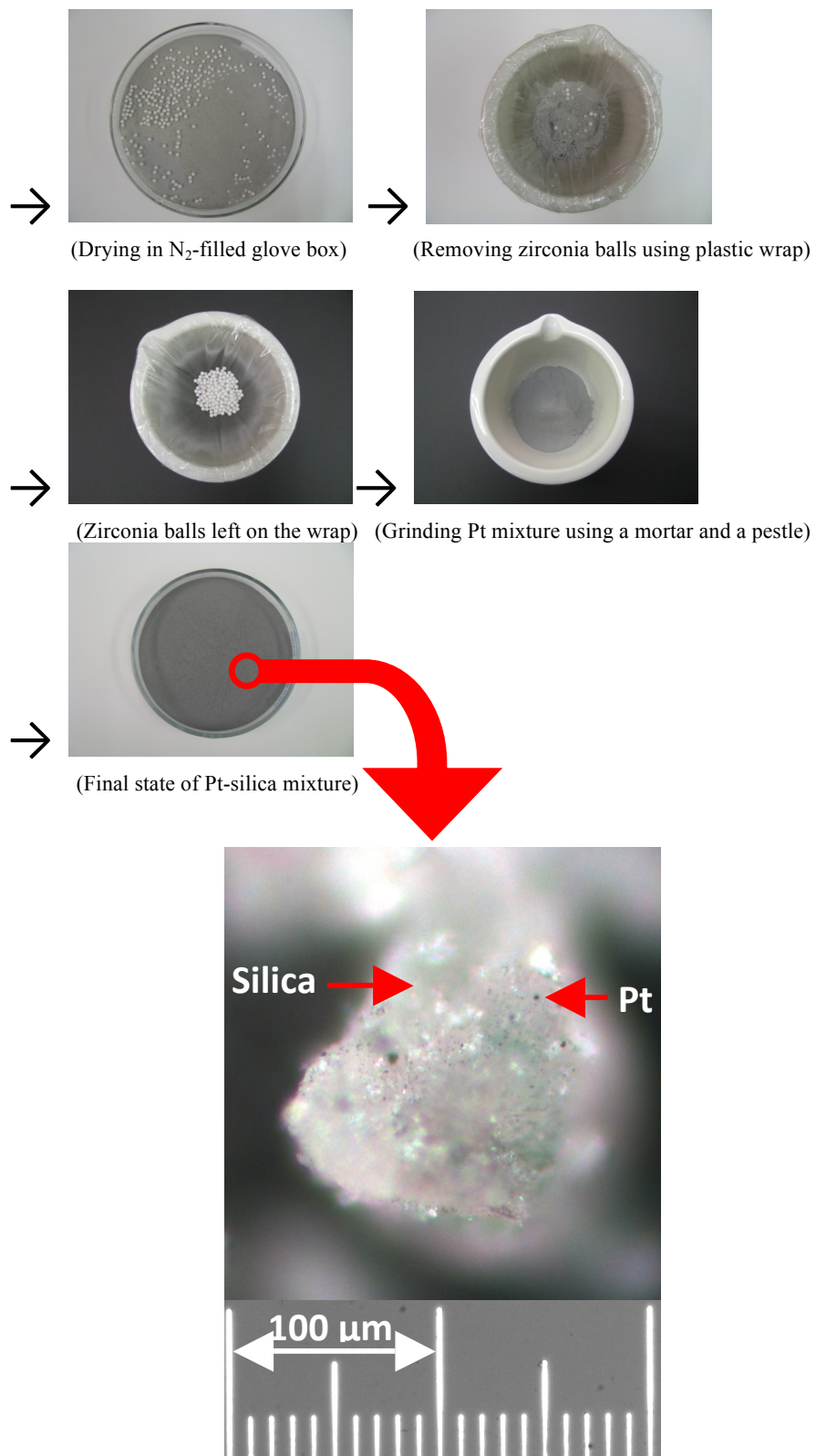
Figure 4.2: Final catalyst mixture preparation and the mixture under the microscope

(Glass wool)

(Quartz reactor)

(Half-packed reactor)

(Glass funnel)

(Reactor placed on the supporting frame)

(Catalyst mixture)

(Fully-packed reactor)

(Narrow section filled with catalyst mixture)
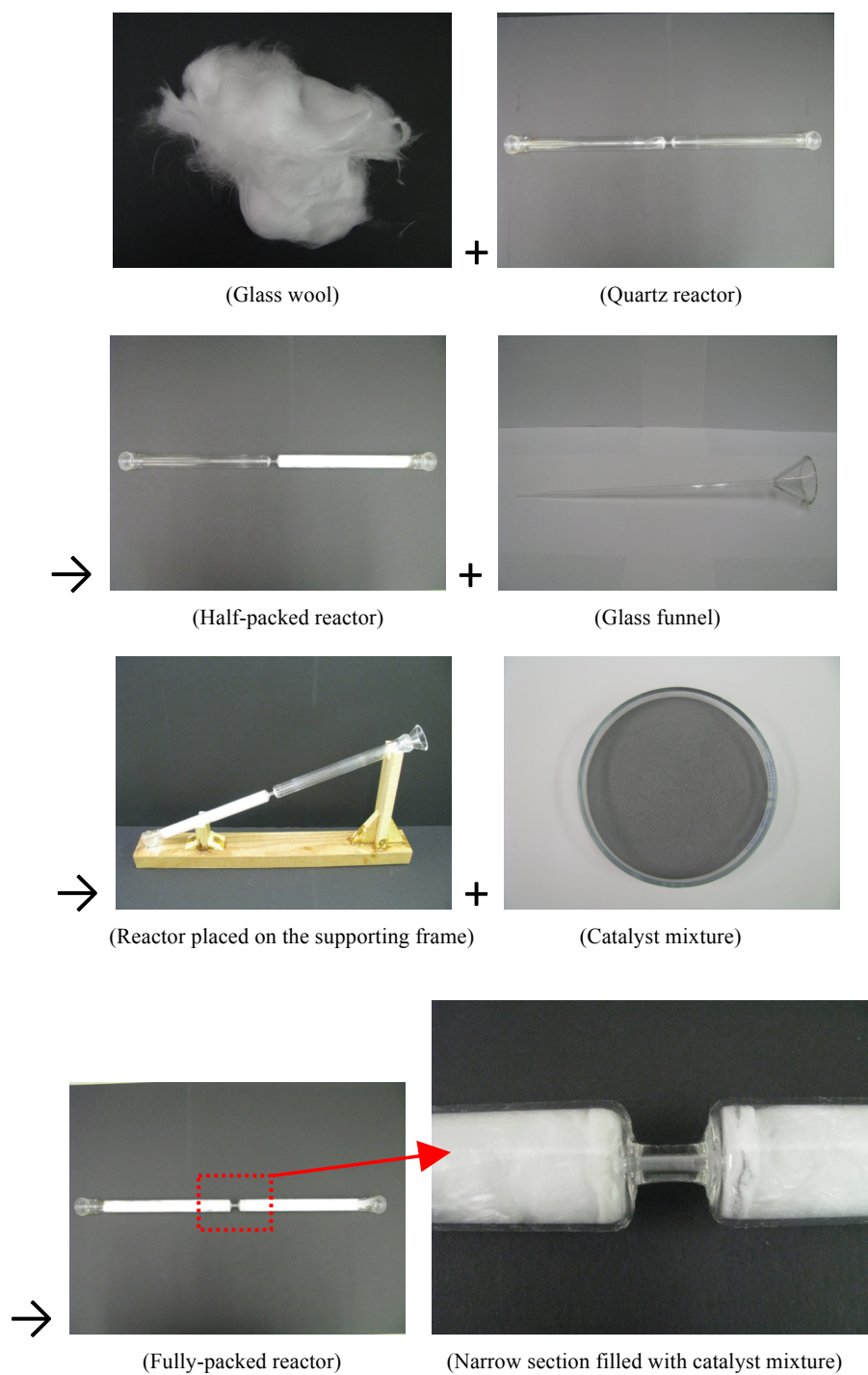
Figure 4.3: Catalyst packing procedures and enlarged narrow section filled with mixture
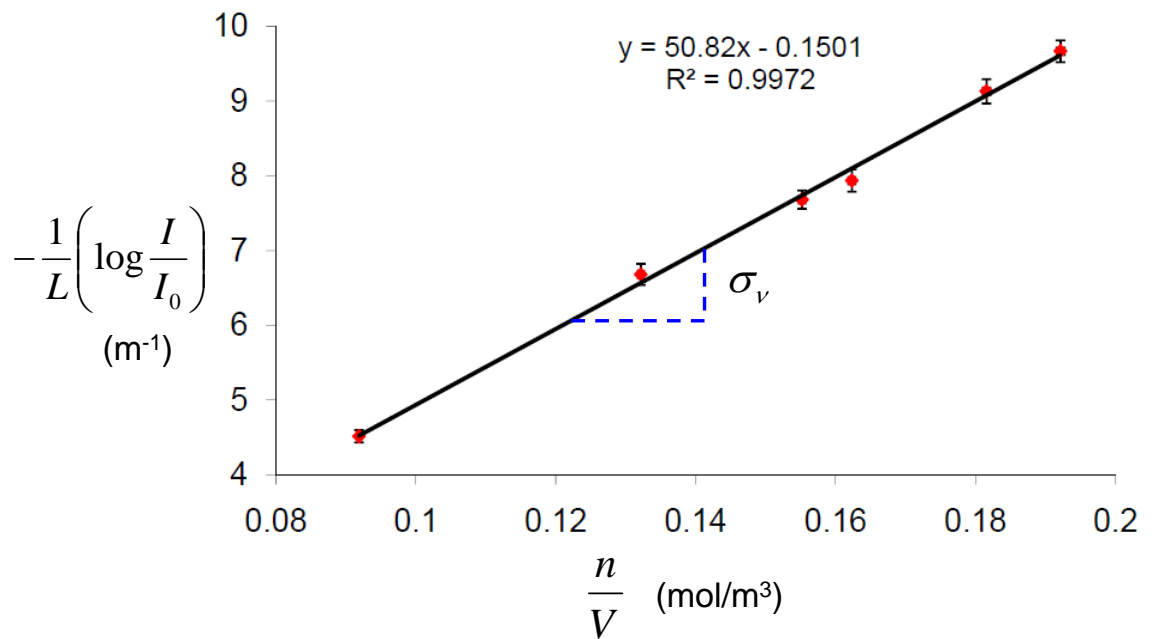
Figure 4.4: Logarithmic plot of the intensity ratio versus fuel concentration, with the slope equal to the absorption cross-section

Chapter 5

Results and Discussion

5.1 Calibration

For calibration of the experiment, the fuels n-octane (C_8H_{18}) and n-nonane (C_9H_{20}) were selected because their vapor pressure is just high enough to have a flammable gaseous mixture at room temperature. Calibration experiments were performed at room temperature and for the temperature range from $125°C$ to $200°C$ because cross-section values at these temperatures are not available in the literature. The results from the tests at room temperature were compared with results from previous studies [10-12].

To calibrate the fuel concentration measurements, a separate test cell was built. The partial pressures of fuel used for the calibration experiments were very low (on the order of 1 Torr), requiring tight tolerances on the leakage rates from the vessel over the full temperature range under investigation. Since the tests were performed at elevated temperatures, the o-rings had to be replaced after every experiment due to the plastic deformation caused by thermal expansion. Additionally, the vacuum grease used, Apiezon H (M&I Materials Ltd.), was found to absorb hydrocarbon molecules and was replaced by Krytox grease by Dupont. All components of the calibration cell including the precision pressure transducer and septum connection were heated and insulated to avoid thermal gradients and fuel condensation.

In the original test procedure, the intent was to measure the absorption cross-section of a fixed amount of fuel as the temperature is increased. However, due to the high thermal expansion coefficient of the test cell, leaks caused by thermal expansion were sufficient to change the amount of fuel over the time required for heating. For successful calibration, the temperature instead was increased while evacuating the test cell and several measurements were taken with different amounts of fuel at each temperature, with each measurement completed within 1 minute. The measured cross-section versus temperature from the current work and the values from previous work [10-12] are shown in Figures 5.1 and 5.2 for n-octane and n-nonane, respectively. The measurement data at selected temperatures is also given in Appendix A.
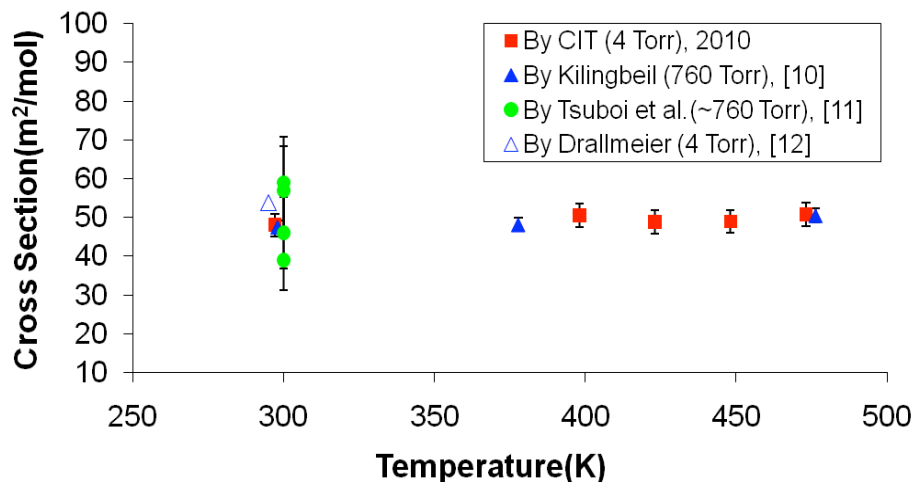
Figure 5.1: Cross-section of n-octane as a function of temperature.
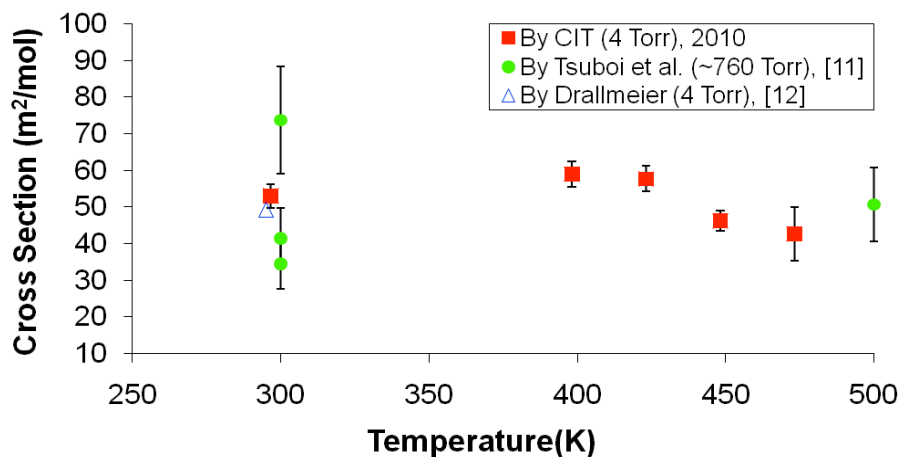
Figure 5.2: Cross-section of n-nonane as a function of temperature.

5.2 Catalytic Modification

A series of validation tests were performed first to verify the use of the measurement techniques. In the test configuration, sapphire observation windows were attached to tubes that branched from the main flow section (see Figure 3.15). Due to the line integration of the laser-based measurement, uncertainty in the fuel concentration may arise from separated or recirculating gas flow. Preliminary tests were conducted using the same gas flow rates used in the main test series to determine whether recirculation was an issue.

The test was initiated with nitrogen flowing through the reactor to obtain a baseline reading. Then, the flow was redirected through the fuel bath, and the subsequent rise time in the fuel concentration was measured. To confirm that no recirculation was occurring, the flow was then changed back to the inert gas, and the fall time of the fuel concentration was measured. The

rise and fall times were consistent, indicating that recirculation does not cause uncertainty in the measurement of the fuel concentration.

While it was determined that no recirculation was present in the flanges, it was noted that during a tests with long durations (greater than 3000 seconds) condensation occurred on the windows. As a result, a heating system was added to the flanges, successfully eliminating the fuel condensation issue. Still, the flanges were cleaned every 4 tests with dish detergent to remove fuel droplets and were rinsed with acetone and isopropyl alcohol.

5.2.1   Effect of Packing the Reactor on the Flow Rate

Packing the reactor with silica or a catalyst mixture blocks the gas flow and causes a pressure rise upstream of the narrow section. At high enough flow rates, the silica or catalyst mixture particles were pushed out of the narrow section and consequently spread throughout the glass wool. To avoid this failure mode, flow rates were kept below 0.7 L/min. Additionally, the blockage created by the tightly packed silicon and catalyst significantly hindered the overall flow through the reactor. This effect was observed in the delay between the detection of fuel in the inlet and outlet flanges, which was on the order of several minutes in some experiments. Starting with the simplest case, an empty reactor, several tests were performed by adding only the components used to pack the catalyst mixture into the reactor to investigate the effects of the packing material on the reaction.

5.3   Empty Reactor with n-Nonane

As a reference case, a test was performed with an empty reactor and a flow rate of 0.5 L/min. The initial furnace temperature was chosen to be 255°C which corresponds to a temperature of 160°C at the outlet flange to prevent the n-nonane from condensing. No reaction occurred at this temperature even when both fuel and oxidizer were present in the flow. When the temperature of the furnace was increased past 310°C, the mole density of fuel at the outlet flange dropped, and since there was no oxidizer, just nitrogen, in the flow this disappearance of fuel molecules was due to pyrolysis. When air flow was supplied at 1250 seconds after the furnace reached 500°C, the mole density of the fuel at the outlet fell even further, approaching zero. This decrease in the mole density indicated that oxidation of the fuel occurred due to auto-ignition. The temperature increase due to the oxidation was observed at the inlet and outlet. A simple calculation (Appendix B) indicates that the temperature of the outlet flange will increase only slightly after oxidation due to heat transfer because of the low flow rate and relatively large diameter of the reactor. To confirm that auto-ignition was indeed occurring, the air supply was stopped and the fuel mole density returned to the original value associated with pyrolysis. After turning off the fuel supply, the mole density values returned to zero at both the inlet and outlet, indicating that were no remnant fuel molecules in either flange.

When the gas was switched between air and nitrogen, spikes appear in the temperature histories which are due to peaks in the flow rate produced by the mass flow controllers. The negative values of the fuel concentration at the outlet after turning off the fuel supply were a result of a change in the baseline laser light intensity I_0 (see Equation 4.3).

Figure 5.3: Variation of fuel molar density and temperature at the inlet and outlet flanges for n-nonane in the empty reactor

5.3.1 Reactor Filled with Glass Wool

In the second set of tests, the reactor was filled with Pyrex glass wool, except for the narrow channel section in the center. As with the reference tests, the flow rate was set at 0.5 L/min. Since the Pyrex has low thermal conductivity, the gaseous fuel does not absorb sufficient heat while in the reactor to trigger pyrolytic reaction. Therefore, the molar density of the fuel at the inlet and outlet flanges remained the same up to a time of approximately 1100 s. At this point in time, the supplied air had been heated to 500°C and this temperature was high enough to cause auto-ignition of the fuel-air mixture. The oxidation is not reflected in the temperature trace because the glass wool disperses the flow and absorbs the heat produced by the oxidation.

Figure 5.4: Variation of fuel molar density and temperature at the inlet and outlet flanges for *n*-nonane in the reactor filled with glass wool

5.3.2 Reactor Filled with Glass Wool and Silica

For the third set of tests, the narrow channel in the middle of the reactor was filled with 0.176 g of silica powder and the rest of the channel was filled with glass wool. For these tests the flow rate was reduced to 0.3 L/min, and a delay of the flow from the inlet to outlet flanges was observed when the fuel supply was turned on and off. This delay was a result of tightly packing the narrow channel in the reactor with the silica particles which are several hundred microns in diameter. The delay in the flow increases the residence time of the fuel in the reactor, and the fuel heats up sufficiently for pyrolysis to occur. The pyrolysis is reflected in the observed disappearance of fuel molecules at the outlet flanges from 700 s to 1100 s when there was just nitrogen and fuel. When air was supplied at 1200 s and the furnace was at 500°C, once again auto-ignition of the fuel occurred. When nitrogen was supplied again at 1900 s, the catalytic oxidation disappeared and only catalytic pyrolysis occurred after 2500 s. At that time, the reaction rate was smaller than the previous pyrolysis that occurred from 700 s to 1100 s as indicated by the elevated fuel concentration. More analysis is needed to understand this phenomenon. Because of the glass wool, the temperature increase due to the combustion is not as large as in the empty reactor. Temperature changes are also observed at the inlet flange when switching between gases because the silica particles delay the flow, increasing the flow temperature.
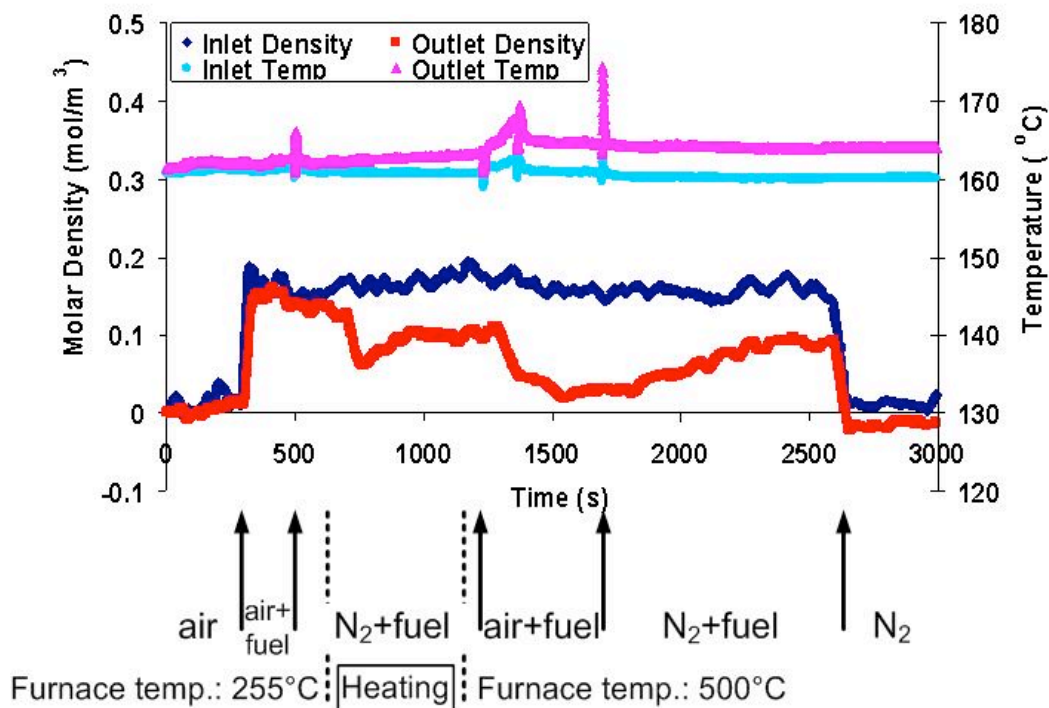
Figure 5.5: Variation of fuel molar density and temperature at the inlet and outlet flanges for *n*-nonane in the reactor filled with glass wool and silica

5.3.3 Reactor Filled with Glass Wool, Silica, and a Platinum Catalyst

In the final set of tests, a mixture of silica and 0.155 g of a platinum catalyst was placed in the narrow channel. The flow rate was again set to 0.3 L/min. To differentiate between pyrolysis and oxidation, only nitrogen was used initially. A slight difference in the inlet and outlet fuel concentrations indicated that pyrolysis was occurring at a temperature that did not lead to pyrolysis in previous tests. The platinum catalyst promoted the pyrolytic reaction resulting in catalytic pyrolysis (Muradov, 1998). After approximately 800 s, the flow stream was switched to air and a decrease in the fuel concentration and temperature increase at the outlet indicated that catalytic oxidation was occurring. Consequently, almost all the fuel molecules were consumed by the catalytic pyrolysis and the catalytic combustion. After heating to 500°C, pyrolysis and catalytic oxidation were still observed. However, the heating did not cause a significant change in the difference in the fuel concentrations at the inlet and outlet flanges when compared with the results at 255°C. After approximately 2800 s, the temperature increased, indicating auto-ignition in the reactor which was at 500°C. While the temperature at the outlet increased, the temperature at the inlet decreased. This was due to the sudden oxidation in the reactor drawing the flow upstream, increasing the velocity at the inlet and therefore decreasing the temperature. This large temperature change at the inlet could have lead to significant changes in the value of the cross-section, and so the temperature at the inlet was increased manually.
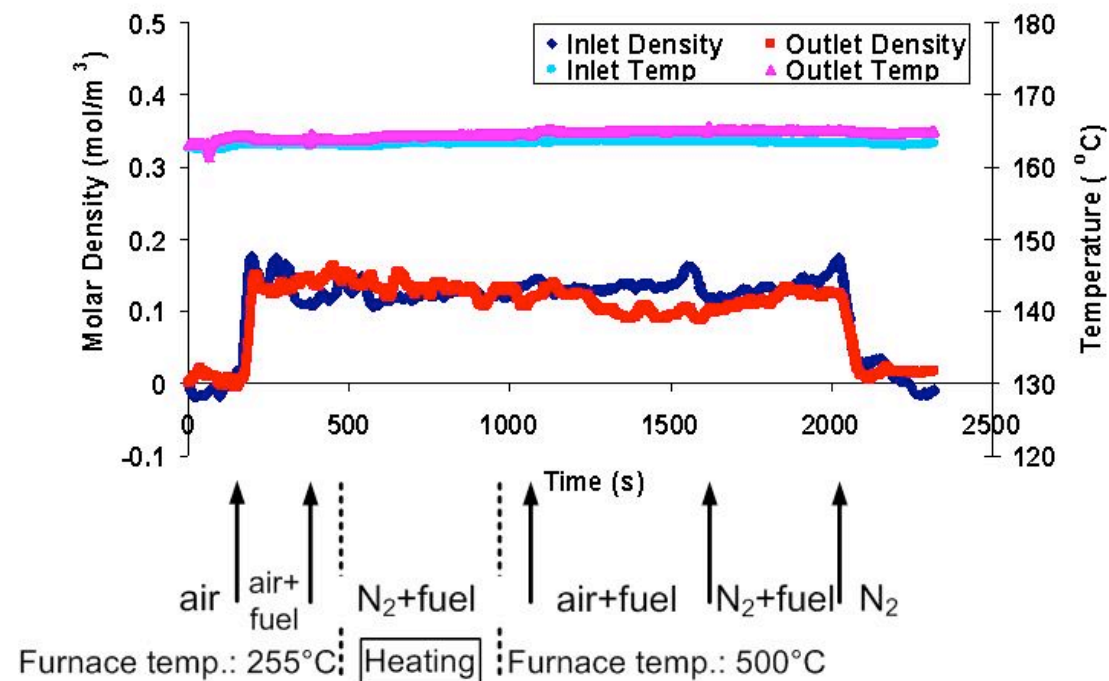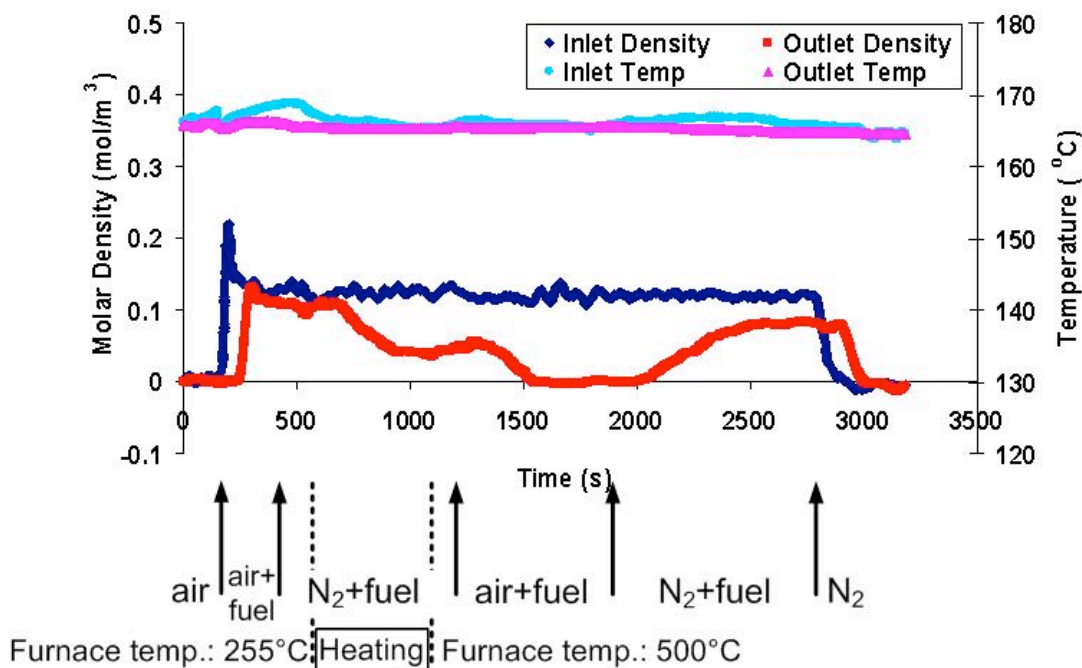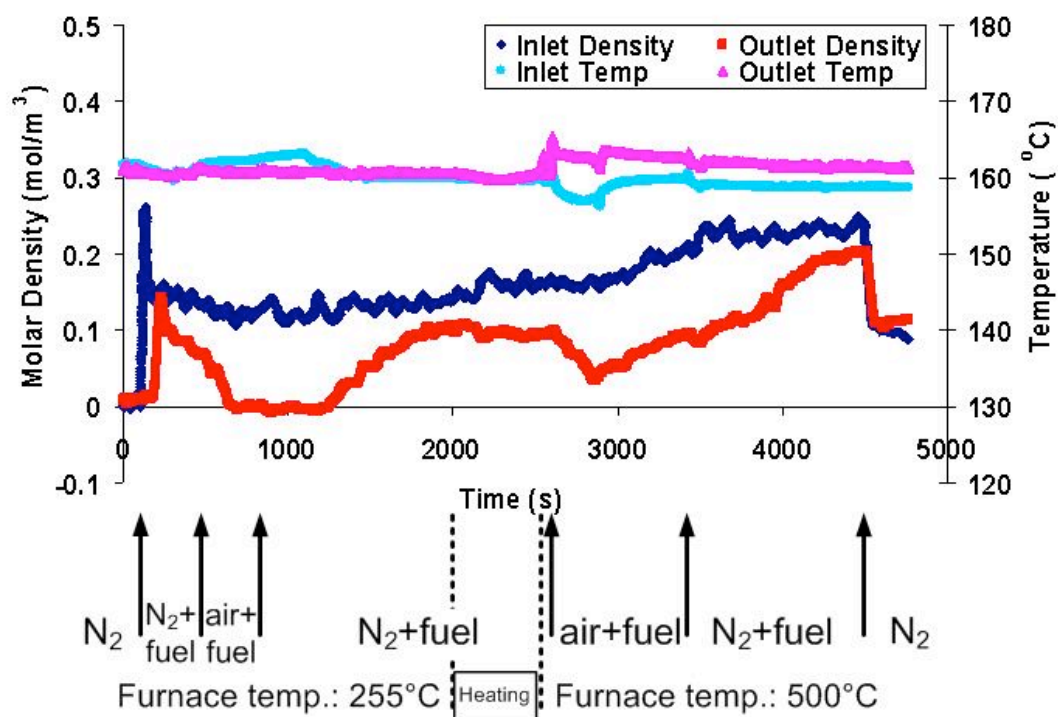
Figure 5.6: Variation of fuel molar density and temperature at the inlet and outlet flanges for n-nonane in the reactor filled with glass wool, silica, and the platinum (Pt) catalyst

Chapter 6

Conclusions

An experimental system was developed to investigate bench-top catalytic combustion with quantitative fuel concentration measurements using laser absorption spectroscopy. The setup included fuel and air supplies and a gaseous fuel generating system to provide flow to a catalytic reactor heated by a furnace. The performance of the system was demonstrated through a series of tests using a platinum catalyst in the reactor.

It was shown that it is possible to lower both the temperature of pyrolysis and oxidation reactions by using the platinum catalyst. While pyrolysis occurred and was measured using the laser diagnostics, the oxidation reactions were the focus of this investigation because they can lower the oxygen concentration below the flammability limit. This initial success in demonstrating catalytic conversion of flammable atmospheres motivates further work on developing catalytic reaction systems for inerting aircraft ullage spaces.

In this study, experiments were performed at two temperatures of the furnace where the catalyst was housed. It is known that catalytic oxidation is strongly dependent on the temperature of the catalyst before the reaction (Lyubovsky et al., 2003). Additionally, catalysts are more reactive under fuel-rich conditions than fuel-lean (Lyubovsky et al., 2003). In the present experiments, the fuel-to-air ratio was held constant (0.5% fuel) because the temperature of the fuel reservoir was fixed at room temperature. Therefore, a parametric study of catalytic oxidation over a range of temperatures and fuel concentrations is required. Finally, it has been shown that the rate of catalytic pyrollysis is influenced by dilution with inert gases (Vasilieva et al., 1991). Therefore, dilution is a potential method to increase the amount of fuel modified through catalytic pyrolysis after the effectiveness of catalytic oxidation is optimized.

Bibliography

Officials eye ground-based inerting to prevent fuel tank explosions. `http://findarticles.com/p/articles/mi_m0UBT/is_29_14/ai_63557904/?tag=content;col1`, July 2010.

Federal Aviation Administration. Reduction of fuel tank flammability in transport category airplanes; final rule. The Federal Register, 73(140), 2008.

National Transportation Safety Board. Aircraft accident report: In-flight breakup over the atlantic ocean trans world airlines flight 800. report AAR-00-03, 2000.

H. S. Gandhi, G. W. Graham, and R. W. McCabe. Automotive exhaust catalysis. Journal of Catalysis, 216:433–442, 2003.

P. Gelin and M. Primet. Complete oxidation of methane at low temperature over noble metal based catalysts: A review. Applied Catalysis B: Environmental, 39:1–37, 2002.

R. E. Heyes and S. T. Kolaczkowski. Introduction to Catalytic Combustion. Gordon Breach Science Publishers, The Netherlands, 1997.

F. P. Incropera and D. P. DeWitt. Introduction to Heat Transfer. John Wiley & Sons, Inc., 3rd edition, 1996.

A. E. Klingbeil, J. B. Jeffries, and R. K. Hanson. Temperature- and pressure-dependent absorption cross sections of gaseous hydrocarbons at 3.39 μm. Measurement Science and Technology, 17: 1950–1957, 2006.

J. M. Kuchta. Investigation of Fire and Explosion Accidents in the Chemical, Mining, and Fuel-Related Industries. Bulletin 680, Bureau of Mines, 1985.

M. Lyubovsky, L. L. Smith, M. Castaldi, H. Karim, B. Nentwick, S. Etemad, R. LaPierre, and W. C. Pfefferle. Catalytic combustion over platinum group catalysts: Fuel-lean versus fuel-rich operation. Catalysis Today, 83:71–84, 2003.

S. C. Moldoveanu. Analytical Pyrolysis of Natural Organic Polymers. Elsevier Science B. V., The Netherlands, 1st edition, 1998.

N. Z. Muradov. Co$_2$-free production of hydrogen by catalytic pyrolysis of hydrocarbon fuel. Energy & Fuels, 12:41–48, 1998.

R. Reid, J. Prausnitz, and B. Poling. The Properties of Liquids and Gases. McGraw-Hill, 4th edition, 1987.

N. A. Vasilieva, R. A. Buyanov, and N. L. Zarutskaya. Dilution effect on catalytic pyrolysis of hydrocarbons. Reaction Kinetics and Catalysis Letters, 45(1):133–139, 1991.

M. G. Zabetakis. Flammability characteristics of combustible gases and vapors. Technical report, Bureau of Mines, 1965. Bulletin 627.

Appendix A

Cross-Section Measurements

Table A.1: Cross section measurement of each fuel at selected temperatures

	σ_ν (m^2/mol)	
T (°C)	n-octane	n-nonane
23	48.04 ± 2.88	52.99 ± 3.18
125	50.48 ± 2.72	58.98 ± 3.54
150	48.85 ± 2.09	57.64 ± 3.46
175	49.00 ± 3.39	46.16 ± 2.77
200	50.82 ± 2.50	42.64 ± 7.25

Appendix B

Heat Transfer Calculations

The equation for calculating the heat transfer to the flow through the pipe under the constant surface temperature condition is (Incropera and DeWitt, 1996):

$$\frac{T_s - T_{m,o}}{T_s = T_{m,i}} = \exp\left(-\frac{pL}{\dot{m}c_P}h\right) \tag{B.1}$$

where the variables are defined as:

T_s: the surface temperature of the pipe

$T_{m,i}$: the mean temperature of the flow at the inlet

$T_{m,o}$: the mean temperature of the flow at the outlet

P: the perimeter of the inside of the pipe

L: the length of pipe from the inlet to the outlet

$\dot{m}$: the mass flow rate

c_P: the specific heat of the gas

h: the convection heat transfer coefficient of the flow
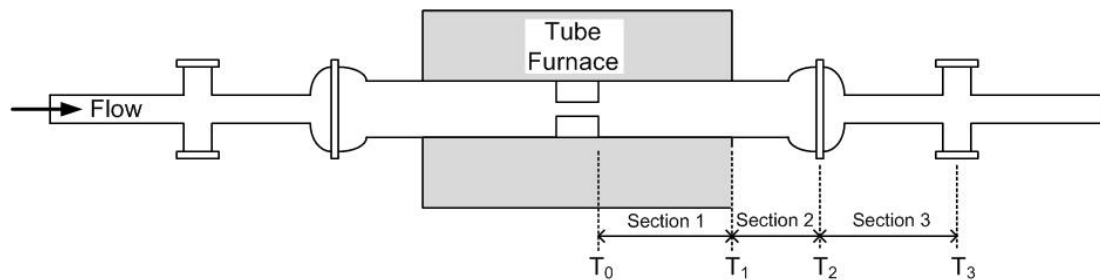
Figure B.1: Reactor schematic for heat transfer calculations

Table B.1: Heat transfer calculation variables

Variable	Section 1	Section 2	Section 3
D [m]	0.021	0.021	0.009
P [m]	0.066	0.066	0.028
L [m]	0.162	0.144	0.181
$\dot{m}$ [kg/s]	9.678×10^{-6}	9.678×10^{-6}	9.678×10^{-6}
c_P [J/kg-K]	1007 for air	1007 for air	1007 for air
h [W/m^2-K]	2	2	2
T_s [K]	773.15	433.15	523.15

Table B.2: Calculated temperature distribution

	$T_0(K)$	$T_1(K)$	$T_2(K)$	$T_3(K)$
Without combustion	773	773	503	516
With combustion	1500	852	519	521

Appendix C

Experiment Checklist

```
Temperature-varying Fuel Density Test
Date:        /          /
Time:
Operator:                                               /

1. Preparation
1) Turn on the fan beside the window. (     )
2) Check if all hand valves are closed. (      )
3) Turn on the circuit breaker 4. (      )
a) Turn on the laser. :            /             (HH/MM)
** 1 hr warm-up is required for the laser source to be stable.
4) Turn on two thermometers in flanges. (      )
5) Turn on the circuit breaker 2 and 3. (      )
6) Turn on the pipe heating control box. (      )
7) Turn on the stirrer & circulating pump for the fuel vessel. (     )
8) Turn on the controllers and start heating. (      )
Zone 1:          C, Zone 2:            C, Zone 3:          C, Zone 4:            C
9) Turn on the flange heating control box. (      )
10) Start heating of flanges. (      )
Inlet:           C, Outlet:            C
11) Start heating of furnace. :            C
12) Flow N2 gas to push out the remnant gas in the piping system.
a) Turn on the MFC A for N2 and the MFC B for air.
   MFC A: (      ), MFC B: (      )
b) Open the hand valves 1, 2, 4 and 8.
```

HV 1: (   ), HV 2: (   ), HV 4: (   ), HV 8: (   )

c) Turn on the Labview program. - 'MFC' (   )

d) Set the flow volume rate.

N2:   SLPM (0.69)

Air: _____   SLPM (0 SLPM because just N2 will be used as a base gas.)

e) Run both MFCs. :   /   (HH/MM)

13) Run the Labview program. - 'Fuel Mod with temp' (   )

a) Turn on the chopper. (   )

b) Open the shutter of the laser source. (   )

c) Check if the laser intensities at two detectors are the same. (   )

d) Check the laser intensity :   (I0, i.e. w/o fuel)

e) Change the value of I0 in the 'Fuel Mod with Temp' to that from step 12-d). (   )

   I0: _____

2. Run

1) Reload the Labview program 'Fuel Mod with Temp' :   _____/_____ (HH/MM)

3. Fuel

1) Check if temperatures arrive at the set values

		Set value (°C)	Present value (°C)
Piping system	Zone 1		
	Zone 2		
	Zone 3		
	Zone 4		
Flanges (By controllers, surface)	Inlet		
	Outlet		
Flanges (By thermometer, gas flow)	Inlet	No set value	
	Outlet		
Furnace			

2) Open the hand valves 3, 5 and 6. :   (s)

HV 3: (   ) ? HV 6: (   ) ? HV 5: (   )

3) Close the hand valve 4. : (   )

4) Check the temperature of fuel. :   C

5) Check the temperatures of gas flow at flanges.

Inlet: C, Outlet: C

4. Air flow

1) Change the flow rate. :   (s)

N2:   SLPM (0)

Air: _____ SLPM (0.69)

2) Check the temperatures of gas flow at flanges.

Inlet: C, Outlet: C

5. N2 gas flow

1) Change the flow rate. :   (s)

N2:   SLPM (0.69)

Air: _____ SLPM (0)

2) Check the temperatures of gas flow at flanges.

Inlet: C, Outlet: C

6. Heating of furnace

1) Start heating of the furnace up to 500 C. :   (s)

2) Check if the temperatures when the furnace is at 500 C. :   (s)

		Set value (ºC)	Present value (ºC)
Piping system	Zone 1		
	Zone 2		
	Zone 3		
	Zone 4		
Flanges (By controllers, surface)	Inlet		
	Outlet		

Flanges (By thermometer, gas flow)	Inlet	No set value	
	Outlet		
Furnace			

7. Air flow

1) Change the flow rate. :   (s)

N2:   SLPM (0)

Air: _____   SLPM (0.69)

2) Check the temperatures of gas flow at flanges.

Inlet: C, Outlet: C

8. N2 gas flow

1) Change the flow rate. :   (s)

N2:   SLPM (0.69)

Air: _____   SLPM (0)

2) Check the temperatures of gas flow at flanges.

Inlet: C, Outlet: C

9. Recovery check (w/o fuel)

1) Open the hand valves 4. (   )

2) Close the hand valves 3, 5 and 6. :   (s)

HV 3: (   ) ? HV 6: (   ) ? HV 5: (   )

3) Check the temperatures of gas flow at flanges.

Inlet: C, Outlet: C

10. Closing

1) Save data. (   )

2) Stop the stirrer. (   )

3) Stop the MFC.

a) Reduce the flow rate as 0. (   )

b) Stop the Labview program 'MFC' and the MFC. (   )

4) Close the hand valve 4. (   )

5) Stop the Labview program 'Fuel Mod with Temp'. (   )

6) Turn off all circuit breakers. (   )